

Effect of Joint Geometry on the Toughness of Epoxy Adhesives

S. MOSTOVOY and E. J. RIPLING, *Materials Research Laboratory, Inc., Glenwood, Illinois 60425*

Synopsis

Increasing joint thickness was shown to increase the toughness of epoxy joints hardened with either tetraethylenepentamine (TEPA) or hexahydrophthalic anhydride (HHPA). The increased toughness was associated with a marked increase in macro-roughness. An upper limit of joint thickness and hence toughness occurred because very thick joints could not be produced. Residual stresses developed during cooling from the curing temperature caused the latter to separate at the interface. Stress corrosion cracking resistance was also found to depend on bond thickness. For the TEPA-hardened system, bond thickness had only a minor influence for thicknesses up to 25 mils; and for the HHPA-hardened system, this persisted to bond thickness of 50 mils. Further increases in bond thickness for both systems caused an abrupt rise in resistance to stress corrosion cracking.

INTRODUCTION

Adhesives used to join rigid adherends are most commonly evaluated by measuring the tensile fracture stress of butt joints, while for nonrigid adherends peel tests are generally used. The former measure of load-carrying capacity is given in units of force/area, e.g., psi in the British system or dynes/cm² in the metric system, while the latter is given in units of energy/area, e.g., in.-lb/in.² or ergs/cm².

One might expect both of these measures of "strength" to be affected in the same manner by the common joint variables, but such is not the case. One of the most important variables in adhesive design is joint thickness, and increasing joint thickness decreases the fracture stress of butt joints, but increases the resistance of joints to peel separation, Figures 1 and 2. This ambiguity leaves unresolved the question of how one might use joint thickness as a design variable to optimize the strength of adhesive. Indeed, in applying laboratory test data to joint design there is the further question of how well these tests model typical service failures. Real structures are flawed in manufacturing; in joints these might be bubbles, dust particles, or unbonded areas, and it is the extensions of these pre-existing flaws that cause complete separation.

Although the peel test is a measure of strength in the presence of a flaw, an analysis of the test is difficult because the energy consumed in forming the

new surface is not distinguished from that used to plastically deform the adherends. The techniques of fracture mechanics, on the other hand, make it possible to define the load-carrying capacities of materials in the presence of flaws in terms of basic material properties that depend only on the energy of separation. Hence, a description of the influence of adhesive variables, and particularly of joint geometry in terms of measurements based on the concepts of fracture mechanics, should be most meaningful in design.

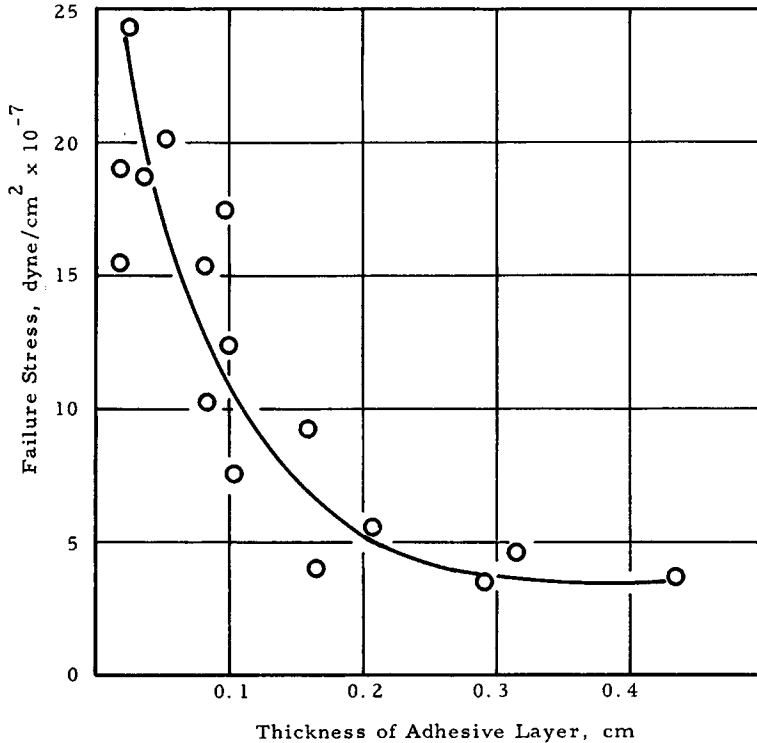


Fig. 1. Effect of thickness of adhesive layer on strength of butt joint. Two 2.32-cm diameter steel cylinders were joined together end to end with poly(methyl methacrylate). Rate of loading was 4.44×10^8 dynes/cm²-sec.¹ (See Ref. 1).

Joints can separate by fast or slow extension of preexisting crack-like flaws. Fast extension occurs at the onset of a load instability at which the crack extension force, or strain energy release rate, has its critical value, G_{Ic} . Slow crack growth in the presence of a sustained load has been shown to be a result of stress corrosion cracking (SCC), with water, in the form of humidity, acting as the corrosive or solvolytic agent.^{3,4} Slow cracking is described by two quantities, $G_{I SCC}$, the value of crack extension force, below which cracks will not extend in the presence of the aggressive environment, and the value of cracking rate, \dot{a} , at values of applied crack extension force, $G_I > G_{I SCC}$.

The purpose of this study was to describe the effect of joint geometry on resistance to both slow and fast crack extension. Resistance to fast fracturing was measured by use of a rising load to obtain the fracture toughness, G_{Ic} , as a function of joint geometry. Resistance to slow cracking was evaluated by measuring \dot{a} versus G_i in a water (plus wetting agent, 0.05 wt-% Kodak Photo-Flo 200) environment. Stress corrosion cracking was conducted in water only, since this was shown to be the limiting cracking rate for relative humidity values approaching 100% at room temperature.³

Two curing agents, i.e., TEPA and HHPA, were used with the single resin, DER 332, to produce the adhesive systems used in the test program.

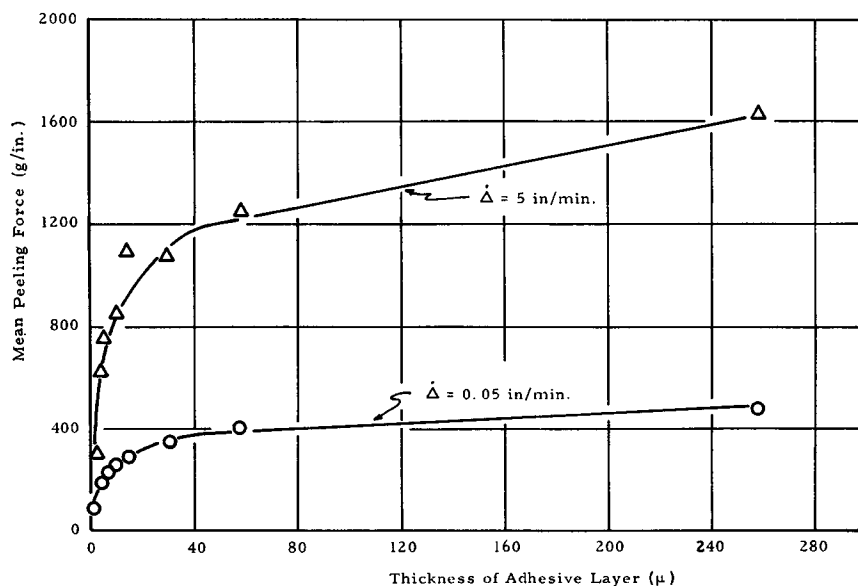


Fig. 2. Dependence of peeling force on thickness of Rhoplex HA-8 layer at two loading rates (Δ = cross-head speed, in./min).²

Three specific compositions were selected on the basis of their rate sensitivity in a rising load test. For the TEPA-cured resin (the room temperature curing system), a rate-insensitive material (10T/180) and a rate-sensitive material (12.5T/280) were used to produce bonds which ranged in thickness from 2 to 250 mils. (Adhesive systems are identified as follows: first number = PHR of hardener; letter indicates hardener type: T = TEPA, H = HHPA; number under slash = postcure temperature (°F).) Since the anhydride curing agent, HHPA, produced bonds which were relatively rate insensitive at all of the compositions and cure temperatures studied, only one system, i.e., 70H/311, was used in the bond thickness study. The range of thicknesses used was similar to that used for the TEPA-cured resin.

head. Thus, the load remains essentially constant as the crack runs so long as the cross-head displacement rate is constant. On stopping and re-loading the specimens, the value of G_{Ic} , which is associated with the critical cracking load, is unchanged. As the joints were increased in thickness, however, the shape of the load extension ($P-\dot{\Delta}$) diagrams was changed. Rather than the load remaining constant after cracking began, two load instability points can be identified; a high value of load at which the crack abruptly jumps ahead at a velocity greater than that dictated by the cross-head velocity, and a lower instability load at which the crack is arrested. The toughness associated with both of these instability points, one for crack initiation and another for crack arrest, are plotted for bond thicknesses of 10 mils or higher.

The dependence of toughness on bond thickness for 10T/180 is quite different from that previously found for another epoxy of unidentified composition (Budd Photostress, Type A).⁶ Whereas the Budd Photostress epoxy displayed a minimum at bond thicknesses between 10 and 100 mils, the TEPA-hardened epoxy showed a maximum in this range. The fracture appearances for the two systems were also quite different. For all thicknesses, Budd Photostress epoxy formed a smooth, highly reflective surface interrupted only by finger-nail marking where crack arrest occurred. Fracturing always occurred near the center of the bond (CoB). The 10T/180 adhesive showed a similar fracture surface for thin bonds, say, 10 mils or less, but at a thickness of about 25 mil the fractures appeared to oscillate, travelling almost from one adherend surface to the other causing a high level of roughness on a macroscale (Fig. 4). The surfaces were still highly reflective, however, indicating a lack of microroughness. Beyond 25 mils, this type of roughening became more general and covered the complete fracture surface. As might be expected, the scatter in toughness measured on a single specimen also increased enormously with the advent of the undulating fracture surface. For bond thicknesses greater than 50 mils, the fracture morphology again changed; bonds of the order of 65 mils or thicker separated adhesively at the adhesive-adherend interface (IF), and, according to Figure 3, this occurred with a continuous loss of toughness. Specimens with bonds thicker than 100 mils could not be manufactured since they separated at the interface during cooling from post-curing.

Although the shape of the G_{Ic} versus bond thickness curves, and the fracture morphology for the 10T/180 joints, cannot be rationalized as yet, it is expected that these effects may be associated with residual stresses developed during curing or possibly with the development of an asymmetric stress field in thick bonds when the crack is near one interface. The latter might explain why cracks wander in thick joints. To determine if the degree of wandering was related to the test configuration, a 50-mil, $m = 4$ in.⁻¹, aluminum adherend specimen was rising-load tested. Initial cross-head rates on this taller specimen matched the rates for the $m = 90$ in.⁻¹ adherends so as to give the same driven cracking rates,⁷ i.e., $\dot{\Delta}$ for

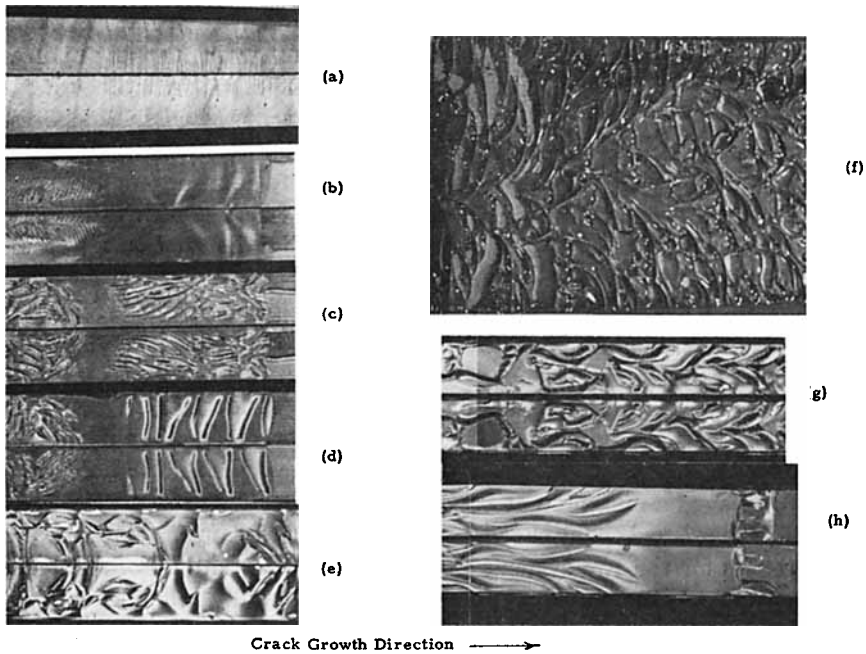


Fig. 4. Fracture morphology of 10T/180 adhesive joints from 10 to 50 mils thickness: (a) 5 mil; (b) 10 mil; (c) and (d) 25 mil; (e), (f), (g), and (h) 50 mil. Specimen (f), 3 in. thick; all others $\frac{1}{2}$ in. thick. Specimens (a) through (e), $m = 90 \text{ in.}^{-1}$; specimen (f), uniform beam, $h = 1 \text{ in.}$; specimen (g) and (h), $m = 4 \text{ in.}^{-1}$. Specimen (h), cross-head rate 10 in./min (high rate fracturing); all others at 1 in./min or equivalent. Note: Photo (a) taken using specular reflection to reveal microripple pattern.

$m = 90 \text{ in.}^{-1}$ is equivalent in terms of driven crack velocity to $\dot{\Delta}/4$ for $m = 4 \text{ in.}^{-1}$. When the taller specimen was run at low rates, \mathcal{G}_{Ic} was 0.86 lb/in. ($\dot{a}_{\text{equiv}} = 1.5 \text{ in./sec}$). For higher rates ($\dot{a}_{\text{equiv}} = 103 \text{ in./sec}$) \mathcal{G}_{Ic} values were of the order of 0.3 lb/in. At the lower rates, the fracture surface was similar to that seen for $m = 90 \text{ in.}^{-1}$ adherends. When the crack was pushed to high rates, the fracture surface became less featured; and at the very high rates, which accompany crack growth from the end of the constant-compliance-change section to the end of the specimen, the fracture was similar in smoothness to thin bonds (Fig. 4).

Increasing the joint thickness might also be thought to decrease the transverse constraint leading to a lower level of plane strain or triaxiality at the crack tip. Hence one thick bond specimen, i.e., 50 mils, was made with 3-in.-wide adherends. So far as constraint is concerned, this would be equivalent to a 5- to 10-mil-thick bond on the normally $\frac{1}{2}$ -in.-wide specimens on which the other data were collected. The toughness of this specimen varied between 0.50 and 0.77 lb/in., which was similar to that found in the narrower, thick-joint specimens, indicating that a decrease in constraint was not causing the higher toughness values. Further, the fracture surface

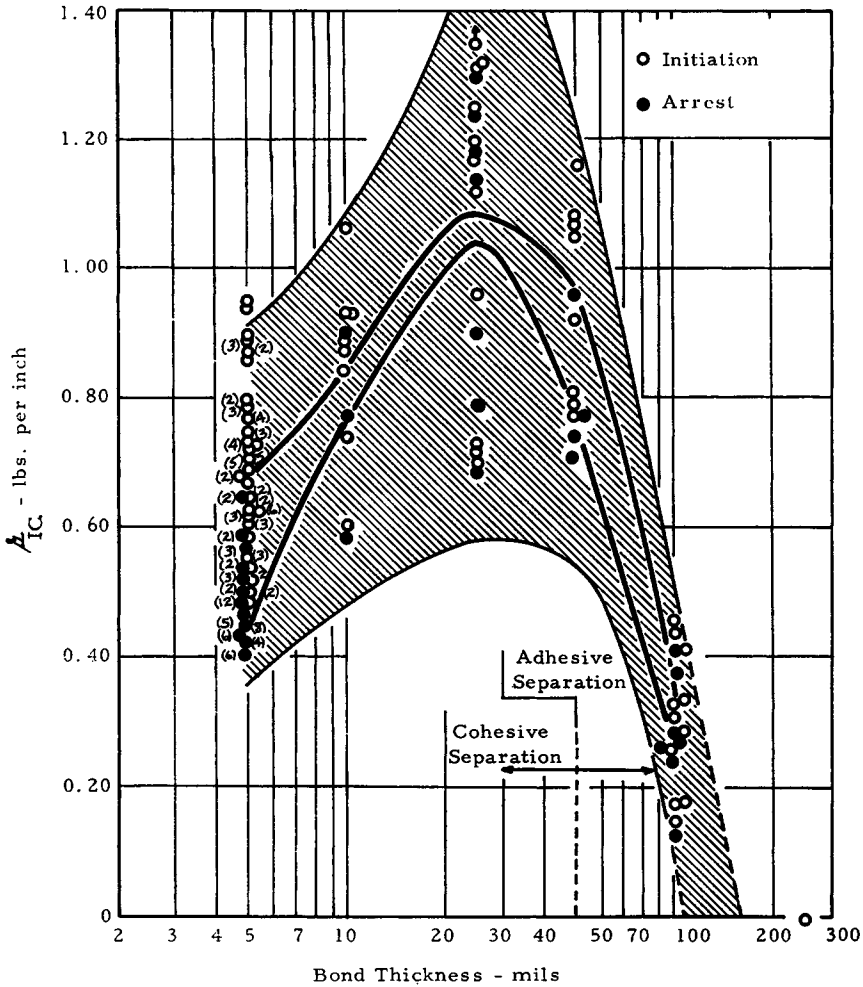


Fig. 5. Effect of joint thickness on toughness of 12.5T/270 adhesive. Cross-hatched area represents 2σ limits and solid curves mean values; upper curve for initiation, bottom curve for arrest. (Numbers in parentheses represent number of tests associated with each data point. Unmarked points are single values.)

for the wider joints showed a pattern of undulations that repeated itself over approximately $\frac{1}{2}$ -in. intervals of width (Fig. 4), suggesting that fracturing occurred over narrow width steps, presumably due to residual transverse shear stresses and the wider area of constraint allowed by the thicker joint.

Increasing load tests were also conducted on 12.5T/270 specimens for bonds of varying thickness (Fig. 5). Again the toughness increased with bond thickness up to approximately 25 mils and then decreased for thicknesses above and below 60 mils. For this more rate-sensitive adhesive, the difference between initiation and arrest was greater than for the 10T/180

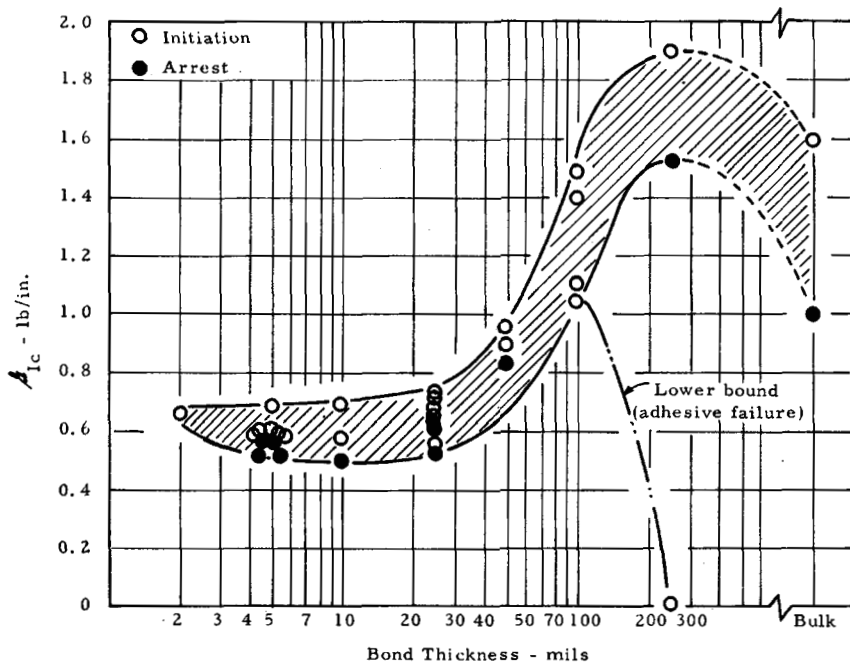


Fig. 6. Effect of joint thickness on toughness of 70H/311 adhesive. All fractures cohesive except lower bound line.

adhesive. Hence, two mean curves, one for initiation and the other for arrest, are shown in Figure 5.

The fracture morphology for 10T/180 and 12.5T/270 were similar: thin joints separated near the center of the bond with very little macroroughness, while the thick bonds again showed undulations. Again, very thick joints separated at the interface.

The bond toughness as a function of joint thickness for 70H/311 is shown in Figure 6. Since less testing was conducted for this adhesive than for the TEPA-hardened resin, the individual points are shown in this figure, not enough data having been collected at most bond thicknesses to establish 2σ limits. The behavior of this adhesive in a rising load test is quite similar to the TEPA-cured material in that increases in thickness resulted in increases in bond toughness. Although for some of the 250-mil-thick joints, IF separation occurred during cooling from postcure, for other specimens such separation did not occur, and these exhibited a continuous rise in toughness to values above those obtained on bulk specimens of identical material. Bulk toughness values for 10T/180 and 12.5T/270 were not available; nevertheless, an extrapolation of data from ref. 3 also indicates that the maximum toughness obtained on the TEPA-hardened joints exceeded the toughness of the epoxy when tested in the bulk form.

Fracturing behavior of the "very thick bond" specimens was a more exaggerated form of that seen for 50-mil bonds with fractures oscillating

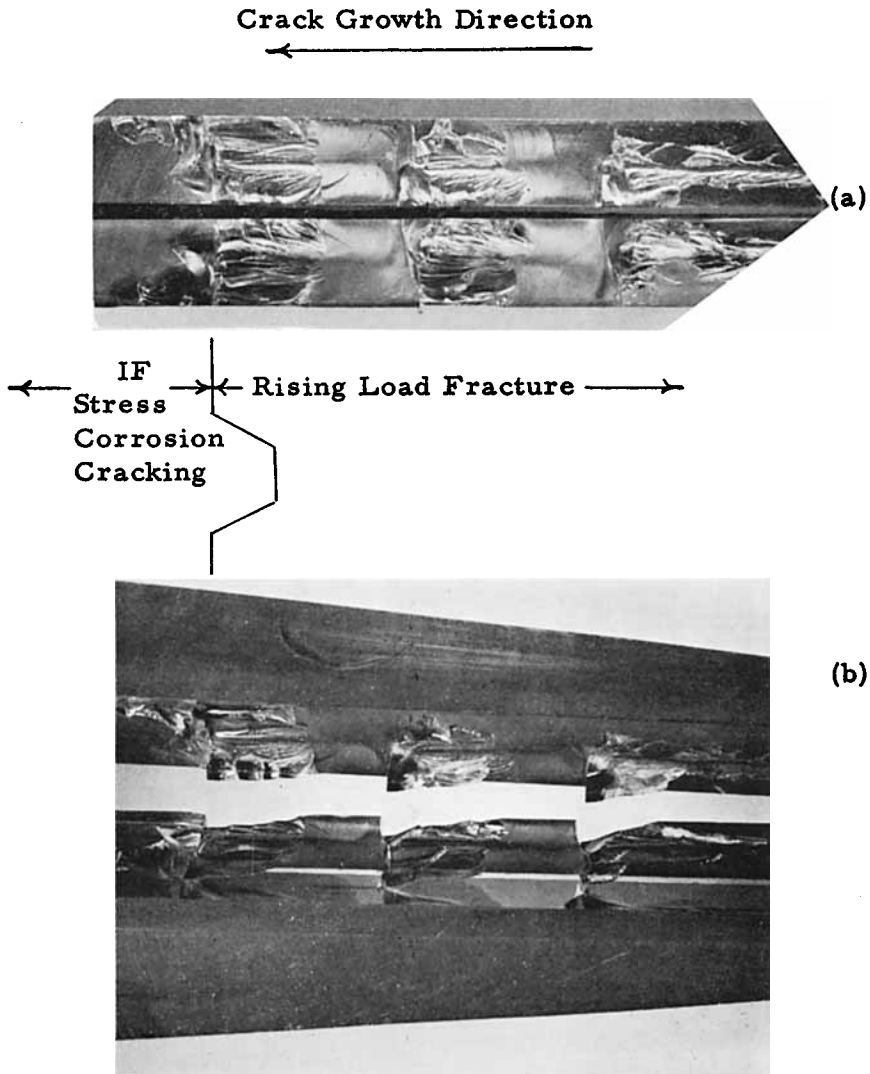


Fig. 7. Fracture surface photographs of 250 mil 70H/311 adhesive bond: (a) top view; (b) oblique view.

from one adherend interface to the other (Fig. 7). Since the values of toughness obtained on bonds thicker than 100 mils can be expected to be higher than bulk only if interface separation can be avoided, a lower-bound line has been added to Figure 6 to show this possibility.

Stress Corrosion Cracking (SCC) Behavior

The stress corrosion cracking tendencies of each of the three adhesive systems were also studied as a function of bond thickness. The de-

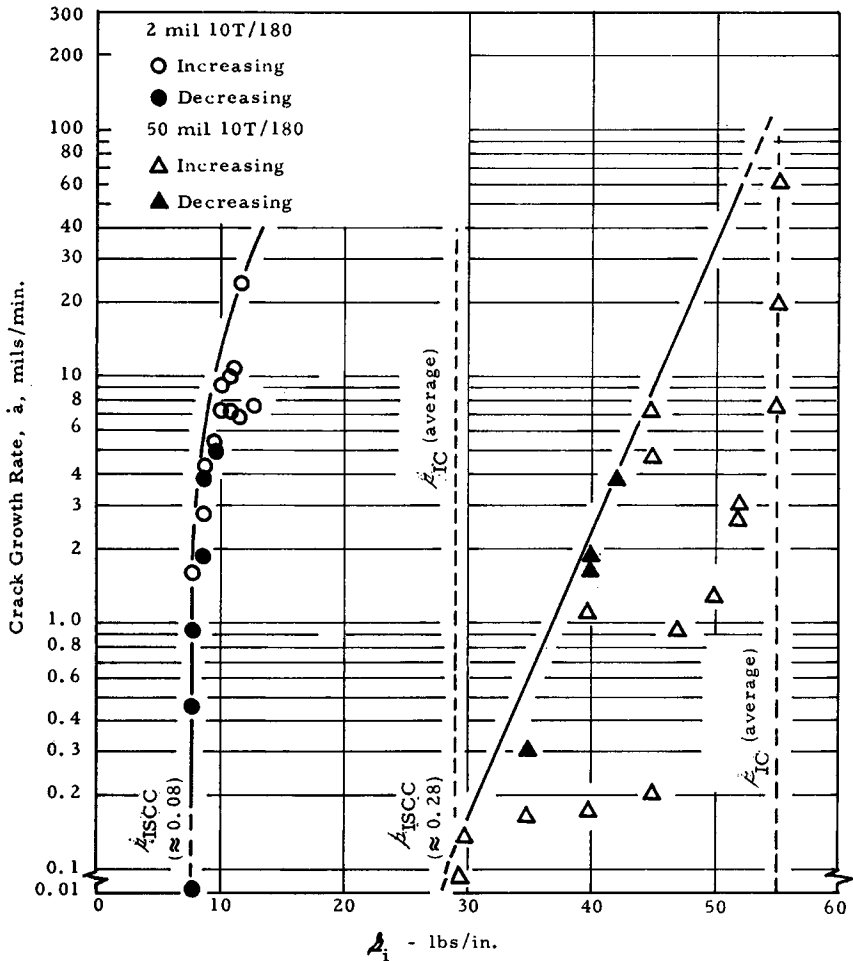


Fig. 8. Stress corrosion cracking of 2-mil and 50-mil 10T/180 adhesive bonds in liquid water.

pendence of cracking rate \dot{a} on applied σ , σ_i , was evaluated in water. Earlier studies³ showed that the cracking rate in water vapor was a function of relative humidity, approaching as its upper limit its value in water containing a wetting agent. Hence, this study was limited to an environment consisting of water plus 0.05 wt-% of Kodak Photo-Flo 200 as the wetting agent. The shape of the \dot{a} versus σ_i curves were identical with those previously described.^{3,7} The scatter obtained on a single specimen with thin joints, however, was less than that obtained on thick ones, as shown for typical 2- and 50-mil-thick joint data in Figure 8.

The value of σ_{ISCC} as a function of bond thickness for 10T/180 is shown in Figure 9a. Between 25 and 50 mils, σ_{ISCC} abruptly increases. Above 100 mils joint thickness, stress corrosion cracking data on TEPA-curve

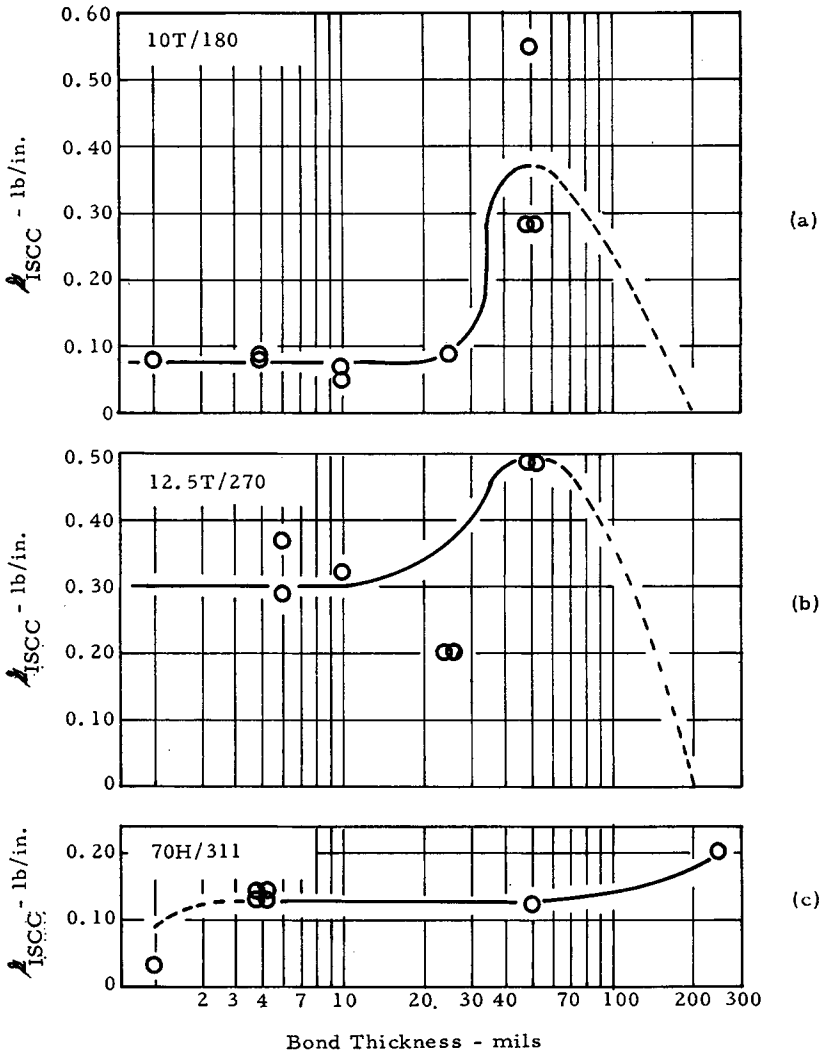


Fig. 9. Effect of bond thickness on $G_{I SCC}$ for three adhesives: (a) 10T/180; (b) 12.5T/270; (c) 70H/311.

adhesive specimens could not be obtained because of the interface separation which occurred during cooling from the postcure cycle.

Similar SCC tests were conducted on 12.5T/270 adhesive specimens, and its cracking characteristics were found to be similar to those of 10T/180, Fig. 9b. The scatter for this material was greater than for 10T/180. Generally, however, the shape of the $G_{I SCC}$ -versus-bond thickness curves were similar, although the effect of joint thickness was less.

It was previously pointed out that fast cracks extend as cohesive failures, i.e., within the bond, while slow cracks in the presence of either liquid water

or water vapor, under low static loads, extend near the interface (IF) and have the appearance of an adhesive failure.³ This change from a cohesive to an adhesive fracture persisted over the complete range of bond thickness from 2 to 50 mils. Since the fracture morphology was unchanged with bond thickness during SCC, the dependence of \dot{a} on G_t for the various joint geometries could not be associated with fracture morphology as was the case for rising load toughness.

The value of $G_{I\text{SCC}}$ versus bond thickness for the HHPA-cured adhesive (70H/311) is shown in Figures 9c. For bond thicknesses up to 50 mils, $G_{I\text{SCC}}$ was essentially constant and increased only between 50 and 250 mils. In spite of this difference in curve shape, the general statement that increased bond thickness leads to increased $G_{I\text{SCC}}$ is still true.

CONCLUSIONS

1. Fracture toughness of low molecular weight epoxy resin adhesives hardened with a polyamine hardening agent (TEPA) increases with increasing bond thickness. The amount of increase, however, is modest so long as the joints crack with the same fracture morphology. Bond thicknesses between 2 and 10 mils fracture near the center of the bond and display very little roughness on a macroscale. At a thickness of approximately 25 mils, the fracture morphology begins to change and the crack oscillates, moving first near one adherend and then near the other, resulting in a high level of macroroughness. This type of fracturing persists from thicknesses of the order of 25 to 50 mils. For the thick joints, the toughness is twice as high as would be expected if the thin bond data were extrapolated to these thicknesses. Bonds thicker than 100 mils could not be produced with the TEPA-cured adhesive since the specimens separated at the adhesive-adherend interface due to stresses developed in postcuring. The high toughness associated with the macroroughening and the degradation of toughness of the thick joints produced a toughness maximum between 10 and 100 mils.

2. The use of an anhydride hardener (HHPA) resulted in similar increases in toughness for increases in bond thickness to 50 mils as described for the TEPA-cured resin. However, for the HHPA system, increasing the bond thickness to 250 mils resulted in a further increase in G_t to above the value for bulk epoxy, as long as the fractures were in the adhesive rather than at the interface. Fracture appearance as a function of bond thickness was similar to that observed on TEPA-cured resin, except that at thicknesses above 100 mils, cracking was even more undulating.

3. An earlier study of the effect of joint thicknesses on an unidentified epoxy, Budd Photostress, Type A, showed a different behavior. The toughness went through a minimum in the range of bond thicknesses between 10 and 100 mils. For the latter epoxy, it was possible to produce joints as thick as 500 mils without either separation during postcuring or the roughening described for both of the other systems discussed above.

Toughness of the thick bonds were approximately equal to the toughness in bulk.

4. The macroroughness and the associated high toughness is thought to be associated with the development of an asymmetric stress field in thick joints and/or residual stresses that developed during cooling from the postcure temperature.

5. The resistance of the bonds to stress corrosion cracking, in terms of G_{rSCC} , also increases with increasing joint thickness. The increase was not continuous with bond thickness, however. Joints between 2 and 25 mils for the TEPA-hardened system showed an essentially constant resistance to stress corrosion cracking, but the thicker bonds (>50 mils) showed a significant improvement in G_{rSCC} . The increase in G_{rSCC} for the HHPA-hardened joints did not occur until the thickness exceeded 50 mils. This improvement was not associated with fracture morphology, since in all cases SCC causes separation at the interface between the adhesive and the adherend.

This program was carried out for the Naval Air Systems Command under the direction of C. Bersch. His many helpful suggestions and those of G. Irwin, Lehigh University, H. Corten, University of Illinois, and R. L. Patrick, Alpha R & D, are gratefully acknowledged.

The specimens were prepared and tested by P. Henderson.

References

1. H. P. Meissner and E. W. Merrill, *ASTM Bulletin*, **151**, 80 (1948).
2. J. L. Gardon, *J. Appl. Polym. Sci.*, **7**, 625 (1963).
3. S. Mostovoy and E. J. Ripling, *J. Appl. Polym. Sci.*, **13**, 1083 (1969).
4. R. L. Patrick, J. A. Brown, L. E. Verhoeven, E. J. Ripling, and S. Mostovoy, *J. Adhesion*, **1**, 136 (Apr. 1969).
5. S. Mostovoy and E. J. Ripling, *J. Appl. Polym. Sci.*, **10**, 1351 (1966).
6. E. J. Ripling, S. Mostovoy, and R. L. Patrick, *ASTM, STP*, No. **360**, 5 (1963).
7. S. Mostovoy and E. J. Ripling, *J. Appl. Polym. Sci.*, **15**, 641 (1971).

Received September 4, 1970